

****FULL TITLE****
*ASP Conference Series, Vol. **VOLUME**, **YEAR OF PUBLICATION***
****NAMES OF EDITORS****

Understanding Infrared Galaxy Populations: the SWIRE Legacy Survey

Michael Rowan-Robinson¹, Carol Lonsdale, Gene Smith, Jason Surace, Dave Shupe, Maria Polletta, Brian Siana, Tom Babbedge, Seb Oliver, Ismael Perez-Fournon, Alberto Franceschini, Alejandro Afonso Luis, David Clements, Payam Davoodi, Donovan Domingue, Andreas Efstathiou, Fan Fang, Duncan Farrah, Dave Frayer, Evanthia Hatziminaoglou, Eduardo Gonzalez-Solares, Kevin Xu, Deborah Padgett, Mattia Vaccari

¹ *Astrophysics Group, Blackett Laboratory, Imperial College London, Prince Consort Road, London SW7 2BZ, UK,*

Abstract. We discuss spectral energy distributions, photometric redshifts, redshift distributions, luminosity functions, source-counts and the far infrared to optical luminosity ratio for sources in the SWIRE Legacy Survey.

The spectral energy distributions of selected SWIRE sources are modelled in terms of a simple set of galaxy and quasar templates in the optical and near infrared, and with a set of dust emission templates (cirrus, M82 starburst, Arp 220 starburst, and AGN dust torus) in the mid infrared.

The optical data, together with the IRAC 3.6 and 4.5 μm data, have been used to determine photometric redshifts. For galaxies with known spectroscopic redshifts there is a notable improvement in the photometric redshift when the IRAC data are used, with a reduction in the rms scatter from 10 % in $(1+z)$ to 5 %. While further spectroscopic data are needed to confirm this result, the prospect of determining good photometric redshifts for the 2 million extragalactic objects in SWIRE is excellent. The distribution of the different infrared sed types in the L_{ir}/L_{opt} versus L_{ir} plane, where L_{ir} and L_{opt} are the infrared and optical bolometric luminosities, is discussed.

Source-counts at 24, 70 and 160 μm are discussed, and luminosity functions at 3.6 and 24 μm are presented.

1. Introduction

Infrared wavelengths hold the key to understanding the evolution of galaxies. From the spectrum of the extragalactic background radiation (Hauser and Dwek 2001) we see that much of the light emitted by stars is absorbed by dust and reemitted at mid and far infrared wavelengths. Only by understanding infrared extragalactic populations can we hope to get a reliable census of the star formation history of galaxies and estimate the fraction of dust-obscured AGN.

The SPITZER SWIRE Legacy Survey has detected over 2 million infrared galaxies in 49 sq deg of sky (Lonsdale et al 2003, 2004). This will be especially powerful for searches for rare objects and for systematic studies of the link between star formation history and large-scale structure. Reliable catalogues have now been delivered to SSC for all the 6 survey areas (Surace et al 2005).

2. Spectral energy distributions

Rowan-Robinson et al (2005) reported work on optical associations, sed modelling, photometric redshifts and redshift distributions for SWIRE sources. To model the sed of SWIRE sources we have used an approach similar to that of Rowan-Robinson et al (2004) for ELAIS sources. The optical data and near infrared data to $4.5 \mu\text{m}$ are fitted with one of the 8 optical galaxy templates used in the photometric redshift code of Rowan-Robinson (2003), 6 galaxy templates (E, Sab, Sbc, Scd, Sdm, sb) and 2 AGN templates (Rowan-Robinson et al 2004). The mid and far infrared data are fitted by a mixture of the 4 infrared templates used by Rowan-Robinson (2001) in models for infrared and submillimetre source-counts: cirrus, M82 starburst, Arp 220 starburst and AGN dust torus. For each of these templates we have detailed radiative transfer models (cirrus: Eftstathiou and Rowan-Robinson 2003, M82 and Arp 220 starbursts: Eftstathiou et al 2000, AGN dust tori: Rowan-Robinson 1995, Eftstathiou and Rowan-Robinson 1995). The approach here is to try to understand the overall SPITZER galaxy population.

Here we report on subsequent work on some interesting samples. Fig 1 (L) shows sed for a sample of SWIRE-ELAIS galaxies for which we have IRS spectroscopy (Perez-Fournon et al, 2006, in prep., Hernan-Caballero et al 2006). Fig. 1 (R) shows sed for a sample of SWIRE-SHADES sources detected at $850 \mu\text{m}$ with SCUBA (Clements et al, 2006, in prep.). For the IRS sample, selected to be bright at $15 \mu\text{m}$, we find that a large fraction of the sources are dominated by an AGN dust torus in the mid-ir. However an interesting subset show PAH features or strong silicate absorption. The $850 \mu\text{m}$ sources show a wide variety of ir templates, including luminous cirrus components, and both M82 and Arp 220 starbursts, as well as several cases dominated by an AGN dust torus in the mid-ir. We also find a wide range of redshifts, with a median redshift of 1.75 and 20% of the sample at $z < 1$.

The striking features that emerge from this modelling are that the sed can at least broadly be understood in terms of a small number of infrared templates. Radiative transfer codes have several parameters and even better fits could be found by using the full range of models of Eftstathiou et al (2000), Eftstathiou and Rowan-Robinson (2003). There is excellent agreement between the IRS and SWIRE data and good consistency with the template predictions.

3. Photometric redshifts in SWIRE-VVDS, Lockman and ELAIS-N1

Rowan-Robinson et al (2005) reported a photometric redshift analysis for two SWIRE samples, the 0.3 sq deg area of Lockman-VF and 6.5 sq deg in ELAIS-N1, based on the methods of Rowan-Robinson (2003), Babbedge et al (2004). Here we show a comparison of $\log_{10}(1 + z_{phot})$ with $\log_{10}(1 + z_{spect})$ for the SWIRE-VVDS sample (Fig 2(L)), which yields over 1300 reliable spectroscopic redshifts for SWIRE galaxies (Lefevre et al 2005, Ilbert et al 2006). and for the whole SWIRE-Lockman area (Fig 2 (R)), in which we have carried out a substantial programme of spectroscopy with Keck, Gemini-N and WIYN (Smith et al, 2006, in prep., Owen et al, 2006, in prep.).

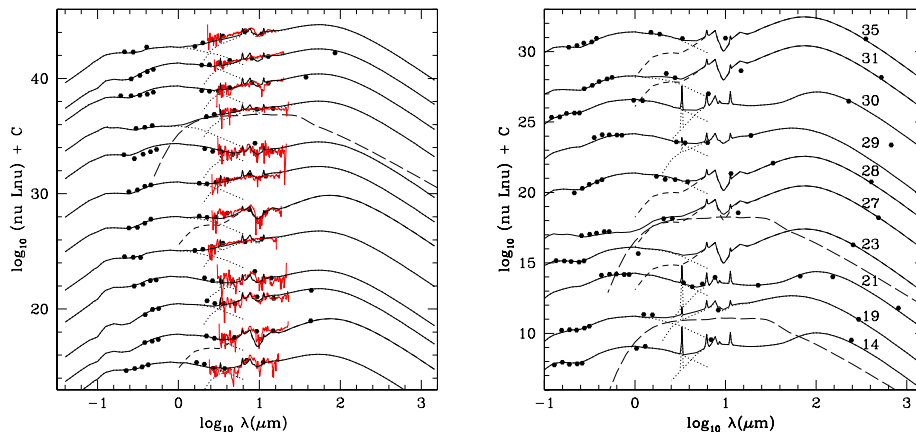


Figure 1. LH: Seds of SWIRE sources with IRS data. RH: Seds of SWIRE-SHADES sources in SXDS.

When including 3.6 and 4.5 μm data in the solution we find accuracies of $\sim 5\%$ in $(1+z)$, compared with 10 % using optical data, and a reduced number of outliers (2%). The number of optical photometric bands is clearly also a factor. For much of the Lockman area we have only gri data available.

4. Redshift distributions

Figure 3 (L) shows the redshift distributions for SWIRE-N1 sources with $S(3.6) > 10 \mu\text{Jy}$, above which the SWIRE survey is relatively complete, with a breakdown into elliptical, spiral + starburst and quasar seds based on the photometric redshift fits. Subsequent to the analysis of Rowan-Robinson et al (2005), we have (1) improved that processing of AGN to include the possibility of QSOs with significant extinction, (2) relaxed the requirements on the code to take account of sources with very weak or no optical data (by using IRAC 5.8 and 8 μm data for these sources). For comparison we show in the top panel the predictions of Rowan-Robinson (2001). Ellipticals cut off sharply at $z \sim 1.4$. Spirals also cut off at ~ 1.5 but there is an extended tail of sources to $z \sim 4$. 10% of SWIRE galaxies have $z > 2$ and 4% have $z > 3$.

The photometric estimates of redshift for AGN are more uncertain than those for galaxies, due to aliasing problems, but the code is effective at identifying Type 1 AGN from the optical and near ir data. For some quasars there is significant torus dust emission in the 3.6 and 4.5 μm bands, so inclusion of these bands in photometric redshift determination can make the fit worse rather than better. We have therefore omitted the 3.6 and 4.5 μm bands if $S(3.6)/S(r) > 3$. Note that only 5 % of SWIRE sources are identified by the photometric redshift code as Type 1 AGN, and of these only 5% are found to have $A_V > 0.5$.

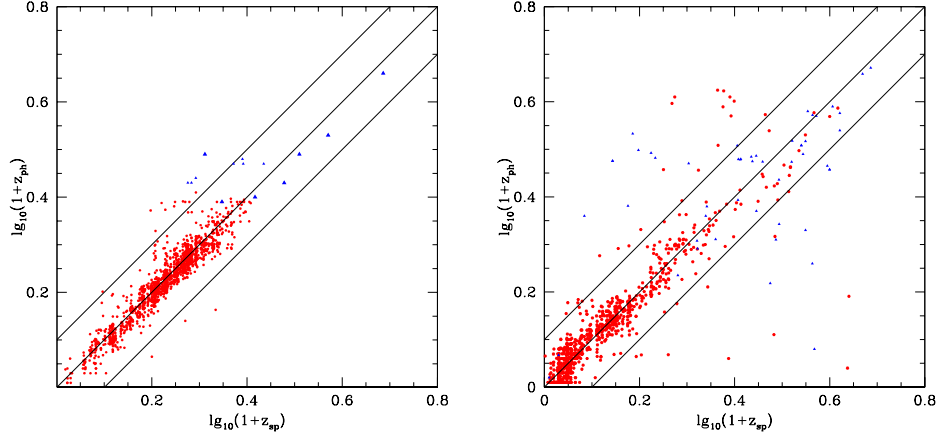


Figure 2. LH: Photometric versus spectroscopic redshift for SWIRE-VVDS sources, showing good accuracy for galaxies out to $z = 1.5$. RH: Photometric versus spectroscopic redshift for SWIRE-Lockman sources.

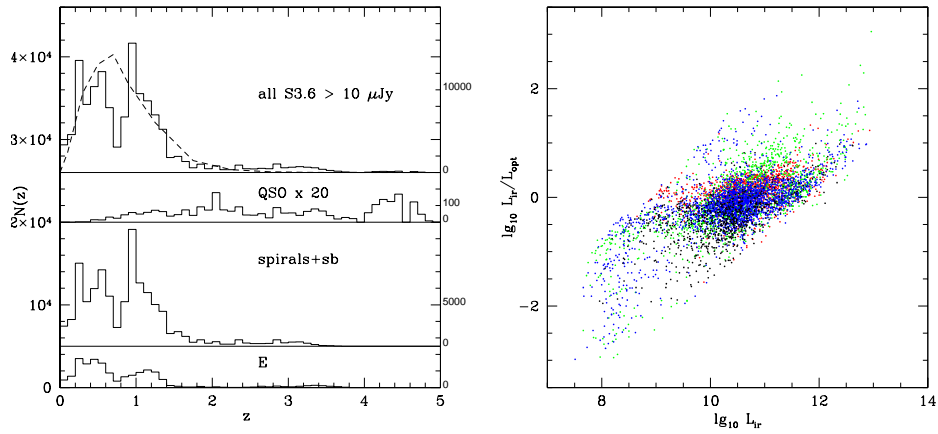


Figure 3. LH: Photometric redshift histogram for SWIRE ELAIS-N1 sources with good 4-band optical IDs, and $S(3.6) > 10 \mu\text{Jy}$. Top panel: all sources, broken curve: prediction of Rowan-Robinson (2001); lower panels: separate breakdown of contributions of ellipticals, spirals (Sab+Sbc+Scd)+starbursts (Sdm+sb), and quasars. The histogram for quasars has been multiplied by 20. RH: L_{ir}/L_{opt} versus L_{ir} for cirrus galaxies, colour-coded by optical template type (black: E, red: Sab, blue: Sbc/Scd, green: Sdm, sb).

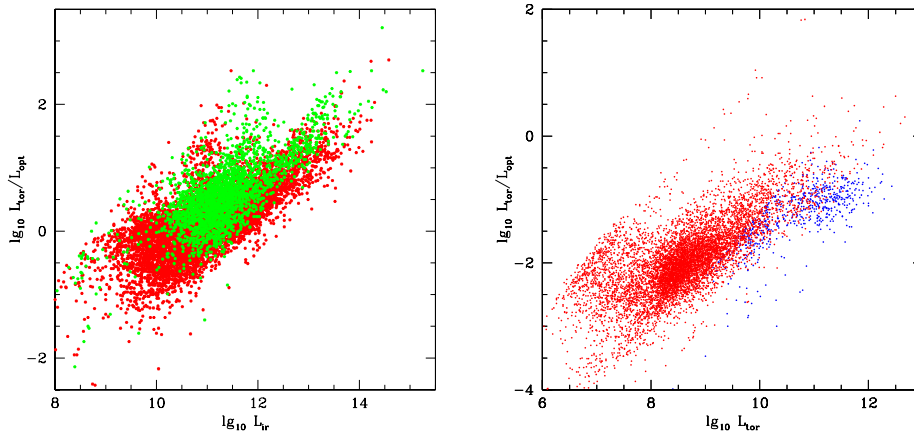


Figure 4. LH: L_{ir}/L_{opt} versus L_{ir} for starburst galaxies (red: M82, green: A220). RH: L_{tor}/L_{opt} versus L_{tor} for AGN dust tori (red: galaxy optical sed, blue: QSO optical sed).

5. Bolometric infrared and optical luminosities

For sources detected at 70 or 160 μm , or with an infrared excess at 4.5–24 μm , relative to the template used for photometric redshift fitting, in at least two bands (one of which we require to be 8 or 24 μm), we have determined the best-fitting out of cirrus, M82 starburst, Arp220 starburst or AGN dust torus infrared templates (cf Rowan-Robinson et al 2005). From the experience of modeling IRAS sources (eg Rowan-Robinson and Crawford 1989), confirmed by the sed modeling described in section 3, we allow (a) a mixture of cirrus and M82 templates, (b) a mixture of AGN dust torus and M82 templates, or (c) an Arp 220 template (using a mixture of AGN dust torus plus A220 template did not improve the χ^2 distribution).

We can estimate the bolometric luminosity corresponding to the infrared template and to the optical template used for photometric redshift determination. Figure 3(R) and 4 shows the ratio of bolometric infrared to optical luminosity, $lg_{10}(L_{ir}/L_{opt})$, versus bolometric infrared luminosity, $lg_{10}L_{ir}$ for cirrus, starburst and AGN dust tori.

For cirrus galaxies with $L_{ir} < 10^{10}L_{\odot}$, a significant fraction of the infrared emission is reemission of starlight absorbed by (optically thin) interstellar dust, so L_{ir}/L_{opt} should be interpreted as the optical depth of the interstellar dust. Many very low values of L_{ir}/L_{opt} (< 0.2) are due to elliptical galaxies with a small amount of star-formation. However there is also an interesting population of luminous and ultraluminous cirrus galaxies, with $L_{ir} > L_{opt}$ (Rowan-Robinson et al 2004, 2005). 7 % of the cirrus galaxies identified in the N1 area have $L_{ir} > 3.10^{11}L_{\odot}$ and 2 % have $L_{ir} > 10^{12}L_{\odot}$. The implications are that (1) the quiescent phase of star formation was significantly more luminous in the past (as assumed in the count models of Rowan-Robinson 2001), (2) the dust opacity of the interstellar medium in galaxies was higher at $z \sim 1$, as expected from

galaxy models with star-formation histories that peak at $z = 1-2$ (Pei et al 1999, Calzetta and Heckaman 1999, Rowan-Robinson 2003).

For star-forming galaxies the parameter L_{ir}/L_{opt} can be interpreted as approximately $10^{-9}\dot{M}_*/M_*(yr^{-1})$, since $L_{ir} \sim 10^{10}\dot{M}_*$ and $L_{opt} \sim 10M_*$, i.e. as $10^{-9}\tau^{-1}$, where τ is the time-scale in yrs to accumulate the present stellar mass, forming stars at the current rate ($\dot{M}_*/M_* = \tau^{-1}$ is the specific star formation rate). The galaxies with Arp 220 templates tend to have high values of L_{ir}/L_{opt} , consistent with the idea that they have lower τ . M82 type starbursts are less extreme and range over rather similar values of L_{ir} and L_{ir}/L_{opt} to the cirrus galaxies.

For AGN dust tori (blue points in Fig 5R), the ratio L_{ir}/L_{opt} can be interpreted (for Type 1 AGN) as the covering factor of the torus. Most have values in the range 0.03-0.5, with a median value ~ 0.1 . If we restrict attention to sources with $L_{ir} > 10^{11}L_{\odot}$, we find that one third have QSO optical sed, while two thirds have galaxy optical seds, implying that the Type 1: Type 2 ratio is 2:1. Further discussion of SWIRE quasars is given by Franceschini et al (2005), Hatziminaoglou et al (2005, 2006), Polletta et al (2006).

5% of 24 μm sources have extremely high infrared luminosities, in the hyper-luminous class ($> 10^{13}L_{\odot}$). Clearly spectroscopy is needed to determine these redshifts more accurately.

The ir templates can be used to predicted fluxes at longer wavelengths. Fig 5 (L) shows predicted fluxes at 70 μm , derived from template fits to 3.6-24 μm data, compared with the observed MIPS fluxes. The agreement is remarkably good. Fig 5 (R) shows predicted fluxes at 350 μm versus redshift for SWIRE-N1 sources.

6. Source-counts and luminosity functions.

Figures 6 and 7 show the differential counts at 24 and 160 μm observed by SWIRE (Shupe et al 2006, Afonso Luis et al 2006), compared with new models developed from the approach of Rowan-Robinson (2001). These new models allow separate rates of evolution for each component; while similar histories are found for cirrus, M82 starbursts and AGN dust tori, the Arp 220 population requires significantly steeper evolution to fit the counts, implying a more dramatic evolution for these extreme objects.

Babbedge et al (2006) have derived luminosity functions at 3.6-24 μm , using the SWIRE-N1 photometric redshifts (Fig 8). The evolution of the 3.6 μm luminosity function is consistent with the passive evolution of starlight, but the evolution at 24 μm implies strong evolution of the star-formation history between $z = 0$ and 1.

References

- Babbedge T. et al, 2004, MN 353, 654
- Babbedge T. et al, 2006, MN subm.
- Calzetti D. and Heckman T.M., 1999, ApJ 519, 27
- Efstathiou A. and Rowan-Robinson M., 1995, MN 273, 649
- Efstathiou A. and Rowan-Robinson M., 2003, MN 343, 322

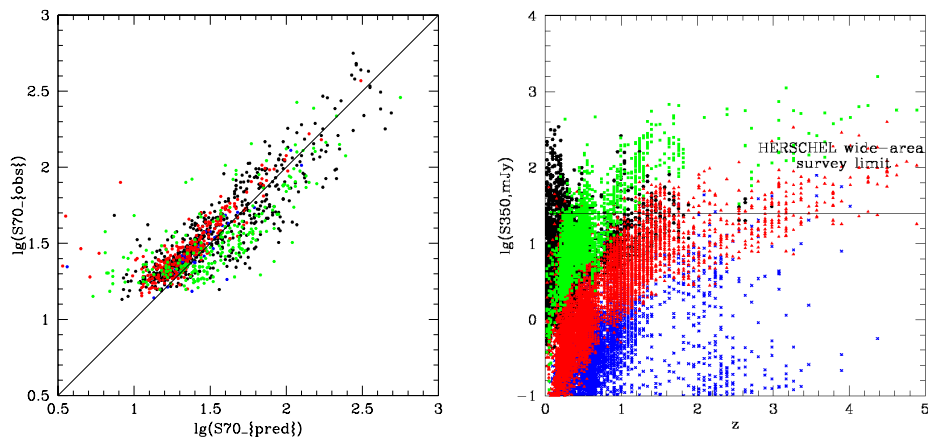


Figure 5. LH: Predicted versus observed 70 μ flux. RH: Predicted 350 μ flux versus redshift for SWIRE-N1 sources. The limit of a planned wide-area survey with HERSCHEL-SWIRE is indicated. Black: cirrus, red: M82 starburst, green: A220 starburst, blue: AGN dust torus.

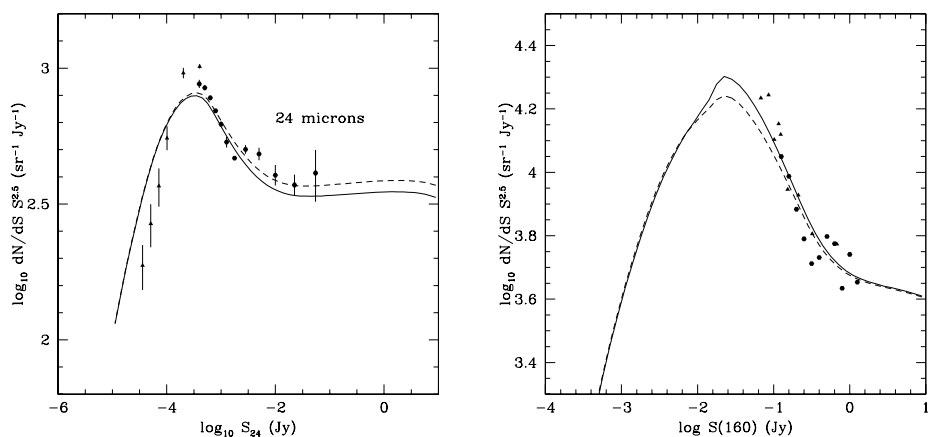


Figure 6. LH: 24 μ differential counts ($mJy^{1.5}deg^{-2}$). RH: 160 μ differential counts ($Jy^{1.5}sr^{-1}$). Filled circles are SWIRE data, filled triangles are from Papovich et al (2004) (LH) and Frayer et al (2006) (RH). The curves are new models based on the approach of Rowan-Robinson (2001).

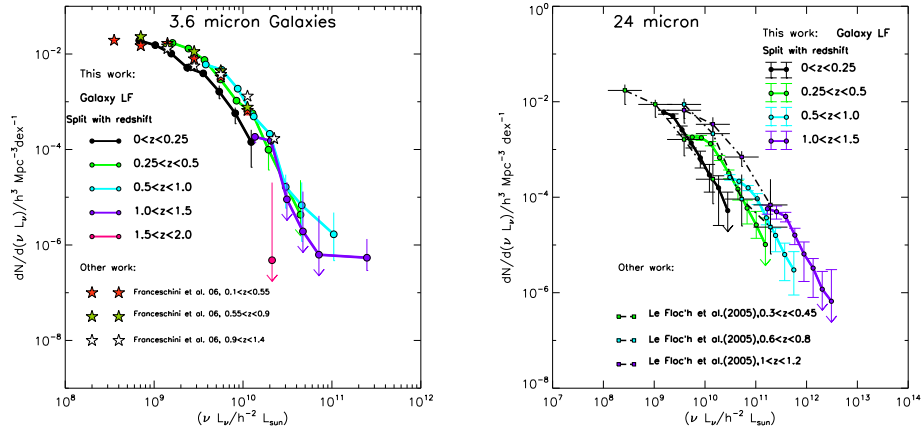


Figure 7. LH: Luminosity function at 3.6 μm for different redshift bins. RH: Luminosity function at 24 μm .

- Efstathiou A., Rowan-Robinson M., Siebenmorgen R., 2000, MN 313, 734
 Franceschini A. et al, 2005, AJ 129, 2074
 Frayer D. et al, 2006, AJ 131, 250
 Hatziminaoglou E. et al, 2005, AJ 129, 1198
 Hatziminaoglou E. et al, 2006, this volume
 Hauser M.G., Dwek E., 2001, ARAA 39, 249
 Ilbert O. et al, 2006, AA (in press), astro-ph/0603217
 LeFevre O. et al, 2005, AA 439, 845
 Lonsdale C. et al, 2003, PASP 115, 897
 Lonsdale C. et al, 2004, ApJS 154, 54
 Papovich C. et al, 2004, ApJS 154, 70
 Pei Y.C., Fall M.S., Hauser M.G., 1999, ApJ 522, 604
 Polletta M. et al, 2006, ApJ(in press), astro-ph/0602228
 Rowan-Robinson M. and Crawford J., 1989, MN 238, 523
 Rowan-Robinson M., 1995, MNRAS 272, 737
 Rowan-Robinson, M., Efstathiou, A., 1993, MN 263, 675
 Rowan-Robinson M., 2001, ApJ 549, 745
 Rowan-Robinson M., 2003, MN 345, 819
 Rowan-Robinson M., et al, 2004, MN 351, 1290
 Rowan-Robinson M. et al, 2005, AJ 129, 1193
 Shupe D. et al, 2006, (subm)
 Surace J. et al, 2005, The SWIRE N1 Image Atlases and Source Lists, SSDC Data Release